Arabinoxylan source and xylanase specificity influence the production of oligosaccharides with prebiotic potential

Carbohydrate Polymers 320 (2023) 121233

Contents lists available at ScienceDirect

Carbohydrate Polymers

journal homepage: www.elsevier.com/locate/carbpol

Arabinoxylan source and xylanase specificity influence the production of oligosaccharides with prebiotic potential

Reskandi C. Rudjito [a], Amparo Jiménez-Quero [a], Maria Del Carmen Casado Muñoz [a], Teun Kuil [b], Lisbeth Olsson [c,e], Mary Ann Stringer [d], Kristian Bertel Rømer Mørkeberg Krogh [d], Jens Eklöf [d], Francisco Vilaplana [a,f,*]

[a] Division of Glycoscience, Department of Chemistry, KTH Royal Institute of Technology, AlbaNova University Centre, SE-106 91 Stockholm, Sweden
[b] Department of Industrial Biotechnology, KTH Royal Institute of Technology, AlbaNova University Centre, SE-106 91 Stockholm, Sweden
[c] Division of Industrial Biotechnology, Department of Biology and Biological Engineering, Chalmers University of Technology, Kemivägen 10, 412 96 Gothenburg, Sweden
[d] Novozymes A/S, Krogshøjvej 36, 2880 Bagsværd, Denmark
[e] Wallenberg Wood Science Center, Chalmers University of Technology, Kemigården 4, 412 96 Gothenburg, Sweden
[f] Wallenberg Wood Science Centre, KTH Royal Institute of Technology, Teknikringen 56-58, SE-100 44 Stockholm, Sweden

ARTICLE INFO

Keywords:
Cereal arabinoxylans
Arabinoxylan structure
Xylanases
Ferulic acid
Prebiotics

ABSTRACT

Cereal arabinoxylans (AXs) are complex polysaccharides in terms of their pattern of arabinose and ferulic acid substitutions, which influence their properties in structural and nutritional applications. We have evaluated the influence of the molecular structure of three AXs from wheat and rye with distinct substitutions on the activity of β-xylanases from different glycosyl hydrolase families (GH 5_34, 8, 10 and 11). The arabinose and ferulic acid substitutions influence the accessibility of the xylanases, resulting in specific profiles of arabinoxylan-oligosaccharides (AXOS). The GH10 xylanase from *Aspergillus aculeatus* (*Ac*Xyn10A) and GH11 from *Thermomyces lanuginosus* (*Tl*Xyn11) showed the highest activity, producing larger amounts of small oligosaccharides in shorter time. The GH8 xylanase from *Bacillus* sp. (*B*Xyn8) produced linear xylooligosaccharides and was most restricted by arabinose substitution, whereas GH5_34 from *Gonapodya prolifera* (*Gp*Xyn5_34) required arabinose substitution and produced longer (A)XOS substituted on the reducing end. The complementary substrate specificity of *B*Xyn8 and *Gp*Xyn5_34 revealed how arabinoses were distributed along the xylan backbones. This study demonstrates that AX source and xylanase specificity influence the production of oligosaccharides with specific structures, which in turn impacts the growth of specific bacteria (*Bacteroides ovatus* and *Bifidobacterium adolescentis*) and the production of beneficial metabolites (short-chain fatty acids).

1. Introduction

Increased consumption of dietary fibres is needed to reach the recommended level of 25 g/day for adults (EFSA Panel on Dietetic Products, N. a. A, 2010). Moreover, the incorporation of dietary fibres and derived oligosaccharides into animal feeds, especially in poultry, is currently being explored to promote their gut health (Aftab & Bedford, 2018; Singh & Kim, 2021). By definition, "dietary fibres are edible parts of plants or analogous carbohydrates that are resistant to digestion and absorption in the host small intestine with complete or partial fermentation in the large intestine" (AACC, 2001). Specifically, dietary fibres that are selectively utilized by host microorganisms causing changes of both the composition and/or activity of the gastrointestinal microbiota, and result in host health benefits are known as prebiotics (Gibson et al., 2017). During fermentation, metabolites such as short chain fatty acids (SFCA) are released by the bacteria and contribute to prevention and control of diseases, such as cardiovascular diseases, gastrointestinal cancer (Kaye et al., 2020; Mendez et al., 2007) and diabetes type II (Delzenne et al., 2015).

Several plant polysaccharides can function as dietary fibres with

* Corresponding author at: Division of Glycoscience, Department of Chemistry, KTH Royal Institute of Technology, AlbaNova University Centre, SE-106 91 Stockholm, Sweden.
E-mail addresses: rudjito@kth.se (R.C. Rudjito), amparojq@kth.se (A. Jiménez-Quero), mdc2@kth.se (M.D.C.C. Muñoz), teun@kth.se (T. Kuil), lisbeth.olsson@chalmers.se (L. Olsson), MSTR@novozymes.com (M.A. Stringer), KBK@novozymes.com (K.B.R.M. Krogh), JEEQ@novozymes.com (J. Eklöf), franvila@kth.se (F. Vilaplana).

https://doi.org/10.1016/j.carbpol.2023.121233
Received 7 April 2023; Received in revised form 13 June 2023; Accepted 22 July 2023
Available online 24 July 2023

potential prebiotic activity. Arabinoxylans (AX) and their hydrolysed products, arabinoxylan-oligosaccharides (AXOS) are examples of dietary fibres that we daily encounter arising from our cereal-based diet. Depending on the plant, tissue of origin and method of extraction used, AXs exhibit distinct molecular structures, differing in the degree, pattern and type of substitutions present (Ebringerová & Heinze, 2000). In cereals, AX is mainly composed of a (1 → 4)-linked-β-D-xylopyranosyl (Xyl*p*) backbone with substitutions of α-L-arabinofuranosyl (Ara*f*) residues at the C(O)-3 and/or C(O)-2 position (Izydorczyk & Biliaderis, 2000). The Ara*f* decorations can be further esterified to ferulic acid (FA) at the C(O)-5 position (Fig. 1b), providing antioxidant properties (Gallardo et al., 2006). Like the carbohydrate constituents, FA can also be released and metabolised by the gut microbiota (i.e. in Bacteroides species), mainly into vinyl phenol derivatives or phenyl propionic acids depending on the bacteria (Pereira et al., 2021; Snelders et al., 2014). Increasing interest has grown towards development of AX and (A)XOS-based prebiotics as highlighted in recent review articles, largely because of their abundance in staple foods, their extractability from cereal processing side streams, and their diversity of molecular structures in terms of substitutions, molar mass and presence of hydroxycinnamic acid decorations (Chen et al., 2019; Lin et al., 2021; Pang et al., 2023; Schupfer et al., 2021; Wang et al., 2020; Zannini et al., 2022). Complex poly- and oligosaccharides have been reported to be more resistant towards degradation, allowing them to be fermented more slowly and to transit further into the distal colon (Snelders et al., 2014; Vardakou, Palop, et al., 2008). This can suppress protein fermentation, which occurs in the distal colon when carbohydrate substrates are depleted. Metabolites from protein fermentation, namely ammonia, *p*-cresol and H_2S, are potentially carcinogenic and thus should be avoided (H. Chen et al., 2015; Diether & Willing, 2019). Different studies show divergent effect of arabinose substitutions on the fermentability of AX and AXOS (Demuth et al., 2021; Rose et al., 2010; Yao, Deemer, et al., 2023; Yao, Flanagan, et al., 2023). Moreover, the presence of bound hydroxycinnamic acids (i.e. ferulic acid) in AX and AXOS seems to hinder fermentability (Demuth et al., 2021; Gong et al., 2019; Li et al., 2023; Snelders et al., 2014). However, a full molecular understanding of the structural features of AX that influence their utilisation by gut bacteria and their prebiotic properties is far from achieved.

(A)XOS are arguably preferred over AX as a prebiotic due to their higher solubility rate and inherently simpler structures, therefore more rapid microbial access for catabolism (Broekaert et al., 2011; Vardakou, Palop, et al., 2008; Zeybek et al., 2020). Conversion of AX into specific (A)XOS with desirable degree of polymerisation and substitution patterns typically involve *endo*-1,4-β-xylanases (xylanase), which cleave the β-1,4 linkage of the xylan backbone. These hydrolytic enzymes are categorised into glycoside hydrolase (GH) families 5, 7, 8, 10, 11, 30 and 43 based on their amino acid sequence (Collins et al., 2005; Henrissat, 1991). Xylanases from GH family 10 and 11 are widely commercialised and much more studied than those from other families. In principle, the GH10 xylanase has the broadest specificity, being able to cleave both

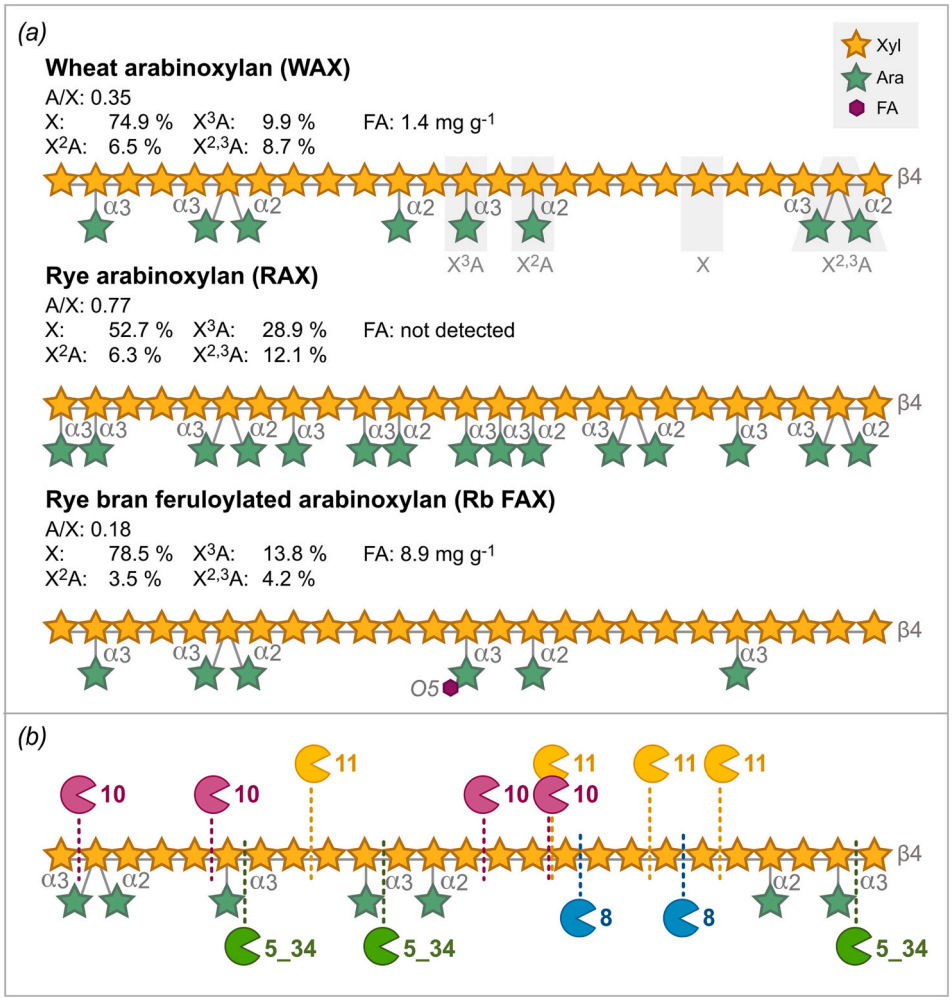

Fig. 1. Arabinoxylan substrates and cleavage sites of xylanases. (a) Structural representation of arabinoxylan (AX) substrates based on monosaccharide and glycosidic linkage analysis. Relative backbone substitution of the AX is shown as the percentage of Xyl*p* that are Ara*f* substituted (X^2A, X^3A, $X^{2,3}A$) and unsubstituted (X). Nomenclature is highlighted in the figure for WAX. Note FA: Ferulic acid. (b) Proposed cleavage sites of xylanases from GH family 11, 10, 8 and 5_34 on AX.

unsubstituted and moderately substituted xylan, with the requirement that at least two consecutive unsubstituted xyloses are present in the backbone for cleavage (Pollet, Delcour, & Courtin, 2010). The *GH11*, on the other hand, preferably cleaves unsubstituted xylan and requires three unsubstituted xyloses for cleavage (Biely et al., 1997; Paës et al., 2012). The GH8 xylanases are less studied but generally prefers linear xylan (Pollet, Schoepe, et al., 2010), while the GH5, particularly those from subfamily 34 (GH5_34) require the presence of arabinose for cleavage (Correia et al., 2011; Labourel et al., 2016) (Fig. 1b). The hydrolysis product of these xylanases on AX will inevitably be a mixture of arabinoxylooligosaccharides (AXOS) and xylooligosaccharides (XOS), collectively known as (A)XOS (Broekaert et al., 2011).

The objective of the present study was to compare the activity of less studied xylanases from families GH8 and GH5_34 with those that are well-characterised xylanases from GH10 and GH11 on different AX substrates. Wheat and rye arabinoxylans substrates were used as starting carbohydrate polymers with differing degrees of arabinose substitution and feruloylation. Using state of the art chromatographic and mass-spectrometric techniques, we analysed the molecular structures of the hydrolysis products in depth, to understand how the different xylanases can tolerate in the active site the presence of arabinose and ferulic acid substitutions in AX. The (A)XOS mixtures were then screened for their prebiotic potential by in vitro anaerobic fermentation of *Bacteroides ovatus* and *Bifidobacterium adolescentis*, along with analysis of their metabolic products. Moreover, by using xylanases from different GH families with distinct canonical specificity towards the presence of arabinose and ferulic acid decorations, detailed information about the intramolecular distribution of substitutions along the xylan backbone could be obtained. This study will broaden our current knowledge on the molecular structure of complex cereal AXs and the production of (A)XOS mixtures employing less-studied xylanase families. These (A)XOS have large potential as additives in food and feed products to improve host gut health.

2. Experimental

2.1. Materials

Wheat arabinoxylan P-ADWAX22 (WAX) and rye arabinoxylan P-RAXY (RAX) were purchased from Megazyme (Wicklow, Ireland). Rye bran feruloylated arabinoxylan (Rb F-AX) was produced in-house using subcritical water extraction (Rudjito et al., 2019), where the rye bran was provided by Lantmännen (Stockholm, Sweden). All the arabinoxylan substrates were characterised in detail and described in the Supplementary material. Arabinoxylan-oligosaccharides comprised of X_2, X_3, X_4, X_5, X_6, A^3X, A^2XX, $A^{2,3}XX$ and XA^2XX/XA^3XX were purchased from Megazyme (Wicklow, Ireland). Bacterial strains *Bacteroides ovatus* (ATCC 8483) and *Bifidobacterium adolescentis* (ATCC 15703) were purchased from the Culture Collection University of Gothenburg (Gothenburg, Sweden). Other reagents were purchased from Sigma Aldrich (Stockholm, Sweden), unless otherwise stated.

2.2. Enzymes

The GH11 *endo*-β-1,4-xylanase from *Thermomyces lanuginosus* (*Tl*Xyn11), GH10 *endo*-β-1,4-xylanase from *Aspergillus aculeatus* (*Ac*Xyn10A), GH8 *endo*-β-1,4-xylanase from *Bacillus* sp. (*B*Xyn8), GH5_34 *endo*-β-1,4-xylanase from *Gonapodya prolifera* (*Gp*Xyn5_34), GH51 arabinofuranosidase from *Meriphilus giganteus* (*Mg*Abf51) and GH43_36 arabinofuranosidase from *Humicola isolens* (*Hi*Abf43_36) were provided by Novozymes A/S (Bagsværd, Denmark). All enzymes were expressed in host strains optimized for heterologous enzyme production. Fungal enzymes (*Tl*Xyn11, *Ac*Xyn10A, *Gp*Xyn5_34, *Mg*Abf51, and *Hi*Abf43_36) were expressed in Aspergillus oryzae and bacterial enzymes (*B*Xyn8) in *Bacillus subtilis*.

2.3. Enzymatic reactions

2.3.1. Enzymatic hydrolysis of arabinoxylan using xylanases

A preliminary pH screening was performed for each enzyme with AZCL-Arabinoxylan to determine the optimal conditions for hydrolysis (Supplementary Material, Method 6). Each enzyme was then tested for the different AX substrates at their optimal pH value (Supplementary Material, Fig. S2). The arabinoxylan substrates were dissolved in either 20 mM acetate buffer (pH 5) or 20 mM phosphate buffer (pH 7) to a concentration of 5 mg/ml. To that, each enzyme was added at 0.01 mg/g or 1 mg/g substrate and the reaction mixtures were incubated at 50 °C for up to 48 h, with agitation. Samples were collected at 0, 1, 3, 6, 17, 24 and 48 h for kinetic analysis. The enzymatic reactions were inactivated at 95 °C for 10 min. For the *Tl*Xyn11, the reactions were either pH inactivated (pH 1–2) by addition of 1 M HCl or filtered through Amicon Ultra Centrifugal Units with a 10 KDa MWCO due to its thermostability. Negative controls were prepared by replacing the enzyme with designated buffer solutions. The reactions were performed in triplicate.

2.3.2. Removal of arabinose using arabinofuranosidase

The inactivated hydrolysate from the 48 h incubation using 1 mg xylanase/g substrate was further treated with *Mg*Abf51 and *Hi*Abf43_36. Each of the arabinofuranosidases were added at 1 mg enzyme/g substrate and incubated at 50 °C for 6 h with agitation. For the hydrolysates that previously used 20 mM phosphate buffer at pH 7, the pH was first adjusted to pH 5 using 1 M HCl before addition of *Mg*Abf51 and *Hi*Abf43_36. The reactions were heat inactivated (95 °C for 10 min) and subjected to OLIMP analysis on the LC-ESI-MS (see Section 2.4.3).

2.4. Product characterisation

2.4.1. Reducing sugar assay

The reducing sugar content was measured using the 3,5-dinitrosalicylic acid (DNSA) assay (McKee, 2017; Miller, 1959) in triplicate, with slight modifications to adapt a 96-well microtiter plate. A standard curve was prepared using xylose solutions with varying concentration from 0.2 to 1.0 mg/ml.

2.4.2. Analysis of oligosaccharides using HPAEC-PAD

The enzymatic reaction mixtures were diluted with MilliQ H_2O and filtered through Chromacol 0.2 μm filters (Scantec Nordic, Sweden). The filtered samples were then analysed using the Dionex CarboPac PA200 column on the ICS3000 system (Dionex Sunnyvale, CA, USA) in triplicate. Separation was achieved using the method described by Falck et al. (2014). Standards of monosaccharides (arabinose and xylose) and oligosaccharides (X_2, X_3, X_4, X_5, X_6, A^3X, A^2XX, $A^{2,3}XX$ and XA^2XX/XA^3XX,) were used as references at 0.005 – to 0.1 g/l.

2.4.3. Oligosaccharide mass profiling (OLIMP)

The oligosaccharide mass profiling was performed using LC-ESI-MS using a Synapt G2 mass spectrometer (Waters Corporation, Milford, MA, USA). Enzymatic hydrolysates were diluted in acetonitrile 50 % (v/v) with 0.1 % (v/v) formic acid to 0.1 mg/ml and filtered through Chromacol 0.2 μm filters (Scantec Nordic, Sweden). Samples were then briefly passed through a ZORBAX Eclipse Plus C18 column 1.8 μm (2.1 × 50 mm) (Agilent Technologies, Santa Clara, CA) for automation and analysed using positive-ion mode in the ESI-MS. The capillary and cone voltage were set to 3 kV and 70 kV, respectively. The oligosaccharides were detected as $[M + Na]^+$ adducts.

2.4.4. Structural determination of (A)XOS using LC-ESI- MS^2

The oligosaccharides were purified using Amicon Ultra Centrifugal Units with a MWCO of 10 kDa, freeze-dried, then chemically labelled via reduction in 2 % borohydride (30 min) and per-*O*-methylation in dimethyl sulfoxide with CH_3I, followed by analysis using LC-ESI-MS^2 (Martínez-Abad et al., 2017). Separation of the reduced per-*O*-

methylated oligosaccharides was achieved using the ACQUITY UPLC HSS T3 column (150 × 2.1 mm, Waters, USA) at a flow rate of 0.3 ml/min with a gradient of a gradient of increasing acetonitrile +0.1 % (v/v) formic acid (10–30 %) over 40 min (Martínez-Abad et al., 2020). Mass spectrometric (MS) analysis was performed in positive mode with the capillary voltage and cone set to 3 kV and 70 kV, respectfully. MS^2 was performed by selecting the ion of interest $[M + Na]^+$ through single ion monitoring (SIM) and subjecting it to collision-induced dissociation (CID) using argon as the collision gas, at a ramped voltage of 35–85 V. Assignation of proposed structures was performed by reference to labelled standards and analysis of the fragmentation spectra using ChemDraw (PerkinElmer, Waltham, Massachusetts, USA).

2.4.5. Size exclusion chromatography

The molar mass of the arabinoxylan substrates before and after hydrolysis were determined using size exclusion chromatography (SEC) fitted with a refractive index detector (Waters, Milford, MA, USA), as described in our previous study (Ruthes et al., 2017).

2.5. Prebiotic potential of (A)XOS produced by different xylanase families

2.5.1. Anaerobic cultivation of gut bacteria in vitro

The prebiotic potential of (A)XOS produced from WAX using the four *endo*-β-1,4-xylanases (Section 2.2) was evaluated on the growth of *Bacteroides ovatus* (ATCC 8483) and *Bifidobacterium adolescentis* (ATCC 15703). (A)XOS produced from the hydrolysis of WAX after 48 h were prepared in a larger batch, freeze-dried, resuspended in water and autoclaved until further use. Inoculum was prepared by activating the bacterial strains in Brain Heart Infusion broth supplemented with 5 g/l L-cysteine, 1 % (*w/v*) hemin, 0.1 % (v/v) resazurin and 2 % (w/v) $NaHCO_3$ solution for *B. ovatus* and MRS broth supplemented with 5 g/l L-cysteine for *B. adolescentis* at 37 °C for 48 h. 1 % (v/v) of the activated inoculum was then inoculated into a screw cap tube containing fermentative media, which consisted of 2 g/l peptone water, 2 g/l yeast extract, 0.1 g/l NaCl, 0.04 g/l KH_2PO_4, 0.04 g/l $MgSO_4.7H_2O$, 0.01 g/l $CaCl_2.6H_2O$, 0.5 g/l L-cysteine hydrochloride, 0.05 g/l hemin, 0.001 g/l resazurin, 2 g/l $NaHCO_3$ and 5 g/l of (A)XOS, WAX or xylose. A layer of paraffin oil was added on top of the fermentative media prior to inoculation. The culture was then incubated at 37 °C for 48 h inside an AnaeroPack Rectangular Jar supplemented with Oxoid AnaeroGen 2.5 l sachets and Oxoid Resazurin Anaerobic Indicator (ThermoFisher Scientific, Stockholm, Sweden). At 8, 24 and 48 h, aliquots of the culture were taken for enumeration in triplicate on Wilkins-Chalgren agar supplemented with 1.5 % agar and 2 % defibrinated horse blood (ThermoFisher Scientific, Stockholm, Sweden) for *B. ovatus* and Reinforced Clostridium agar (Sigma Aldrich, Stockholm, Sweden) for *B. adolescentis*. The plates were incubated at 37 °C under anaerobic conditions for 3–5 days. Colonies formed were counted as colony forming units (CFU/ml). Utilisation of (A)XOS was monitored using the HPAEC-PAD, as described in Section 2.4.2.

2.5.2. Short chain fatty acid profiling

The short chain fatty acids (SCFA) released during fermentation were analysed using the Waters 2695 Separation Module HPLC system coupled to the Waters 2996 photodiode array detector at 210 nm (Waters, Milford, MA, USA) in duplicate. Separation of the organic acids was achieved using the Aminex® HPX-87H ion exclusion column at 60 °C (Bio-Rad, CA, USA) with an isocratic flow of 5 mM H_2SO_4 at 0.6 ml/min (Zeppa et al., 2001). A mixture of acetate, propionate, butyrate as well as pyruvate, lactate, fumarate and succinate were used as references for external standard calibration.

3. Results and discussion

In this study, we investigated the activity of xylanases from different GH families on arabinoxylan (AX) substrates with differing degrees of arabinose (Ara*f*) substitution and feruloylation. Four xylanases, (*Tl*Xyn11, *Ac*Xyn10A, *B*Xyn8 and *Gp*Xyn5_34) were selected and analysed on wheat arabinoxylan (WAX), rye arabinoxylan (RAX) and rye bran feruloylated arabinoxylan (Rb FAX). By performing a direct comparison, we aimed to highlight their key relative differences in activity, in the structure of their hydrolysis products, and their application in prebiotic production. The proposed molecular structure of the AX substrates used in this study is shown in Fig. 1a. Among the three AX substrates, WAX exhibited an intermediary arabinose to xylose ratio (A/X) of 0.35, RAX was much more substituted (A/X: 0.77), while Rb FAX was the least substituted (A/X: 0.18). In terms of phenolic acid substitution, Rb FAX had the highest ferulic acid content at 8.9 mg/g with minor amounts of *p*-coumaric acid at 0.2 mg/g (ESI Table 1). The Rb FAX was extracted using subcritical water, which allowed for the esterified moieties to be preserved and remain covalently linked to the AX core (Ruthes et al., 2017).

3.1. Investigating the specificity of the xylanases with respect to arabinose substitution

3.1.1. General activity in terms of reducing sugar release

The activity of the xylanases on the AXs is inevitably affected by the presence of Ara*f* substitutions. Following end-point incubations, the reducing sugar analysis (Fig. 2a) revealed that the *Ac*Xyn10A was most active on all the AX substrates, inferring that it was active on both linear and highly substituted xylans. The GH10 xylanases feature an open-binding substrate cleft due to its TIM barrel $(\alpha/\beta)_8$ structure and can tolerate arabinose substitution in subsite −2, +1 and sometimes +2. Only at subsite −1 is substitution not accommodated (Fujimoto et al., 2004; Pell et al., 2004; Vardakou et al., 2005). In addition, the GH10 xylanases generally prefer shorter substrates (X_2-X_5) (Linares-Pastén et al., 2018), resulting in the release of even smaller products that attributed to the higher amount of reducing sugars. It should be noted that the reducing sugar assay does not consider the size of the hydrolysis products and thus only provides a general overview of the enzyme activity.

Following *Ac*Xyn10A, *Tl*Xyn11 was the second most active, displaying higher activity on WAX and Rb FAX as compared to RAX. The GH11 xylanases are more restricted to substitution than those from GH10. It adopts a conserved β-jelly roll structure, which resembles a partially closed right hand. The α-helix portion, which depicts the thumb-like structure, results in a narrow binding cleft and limited substitution is tolerated at subsite −2, while no substitution is allowed at subsite −1 and +1. Nevertheless, substitution can be accommodated at subsite −3 and +2 (Paës et al., 2012; Pollet et al., 2009), which explains the *Tl*Xyn11's moderate activity on RAX.

Interestingly, the *B*Xyn8 showed the most restriction towards substitution, exhibiting the lowest activity in RAX and the highest in Rb FAX. Previous studies on GH8 xylanases from *Pseudoalteromonas haloplanktis* and an uncultured bacterium have highlighted their preference towards linear substrates, whereby activity of the GH8 xylanases decreased with increasing degree of substitution. The authors reported that an extended loop in close proximity with the glycone region (subsites −3 and −2) reduced the accessibility for substitutions (Pollet, Delcour, & Courtin, 2010; Pollet, Schoepe, et al., 2010). In contrast to *B*Xyn8, the *Gp*Xyn5_34 much preferred the highly substituted RAX as compared to WAX and Rb FAX. The GH5_34 xylanase requires the presence of a C(O)-3 linked arabinose at the −1 subsite as a specificity determinant for cleavage, as shown by the xylanase from *Clostridium thermocellum* (Correia et al., 2011). The presence of Ara*f* can additionally be tolerated at subsite −4 to +2 as the enzyme adopts an open cleft structure (Falck et al., 2018; Labourel et al., 2016). Such dependence towards Ara*f* substitution explains the low activity of the *Gp*Xyn5_34 towards WAX and Rb FAX.

To elucidate the enzyme kinetic profiles in more detail, a lower

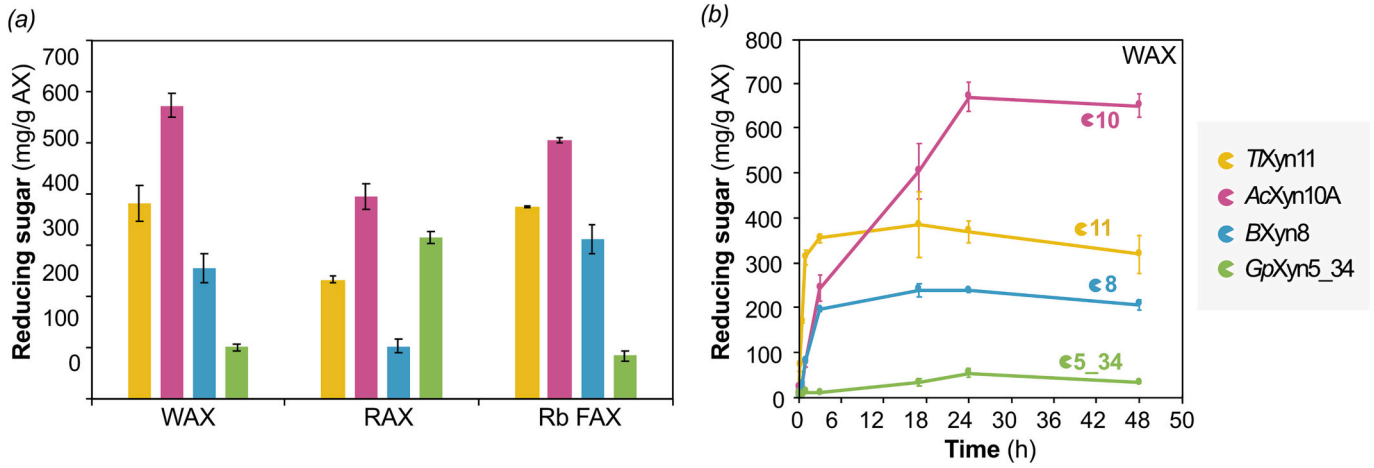

Fig. 2. Activity of xylanases on different arabinoxylan (AX) substrates. (a) End-point measurement of reducing sugars from enzyme activity on WAX, RAX and Rb F-AX (1 mg enzyme / g AX, 48 h, pH optimum) corrected with the negative AX controls for basal reducing sugar content. (b) Temporal measurement of reducing sugars on WAX (0.01 mg enzyme/g AX). Standard deviations are from triplicate reactions. The time activities on RAX and Rb-FAX are shown in ESI Fig. S3.

enzyme concentration (0.01 mg enzyme/g AX) was used while keeping the other reaction conditions the same at the optimal pH. The temporal measurement of reducing sugars, as shown in Fig. 2b and ESI Fig. S3, revealed that the *Tl*Xyn11 hydrolysed all the three AXs at the fastest rate. The *Ac*Xyn10A was the second fastest but resulted in the highest amount of reducing sugars at the end of the incubation, in agreement with Fig. 2a. Meanwhile the *B*Xyn8 was considerably slower especially in RAX, and the *Gp*Xyn5_34 was particularly slow in all the AX substrates and did not reach its end point (in comparison to a higher enzyme load).

3.1.2. *Enzymatic product analysis revealed distinct mono- and oligosaccharide profiles*

The combination of different xylanases and AX substrates used in this study resulted in unique profiles of mono- and oligosaccharides, as shown from the HPAEC-PAD results, whereby peaks that could be assigned to standards were subsequently quantified (Fig. 3). Hydrolysis products of GH10 and 11 xylanases on xylans have been well reported and are generally small in size (Pollet, Delcour, & Courtin, 2010). Here we show that xylose (X_1) and xylobiose (X_2) were the main products of *Ac*Xyn10A and *Tl*Xyn11 (Fig. 3a-d). In the chromatographic profiles of *Tl*Xyn11, result showed the typical hydrolysis products of short linear xylooligosaccharides (XOS) and substituted (A)XOS in the form of XA^2XX and XA^3XX (Fig. 3a-b). Interestingly after 48 h, both X_5 and X_6 were completely hydrolysed, while X_2 increased sharply, as observed in both WAX (Fig. 3b) and Rb F-AX (ESI Fig. S6b). The high abundance of X_2 is rather uncommon for a GH11 xylanase, as their main hydrolytic products are usually one unit longer than those generated by family GH10 xylanases. Nevertheless, high production of X_2 was observed previously from the xylanase of *Thermomyces lanuginosus* (Gomes et al., 1993). A possible contribution for the accumulation of X_2 could be the slight exo-xylosidase activity observed by *Tl*Xyn11 (ESI Fig. S4), which becomes more apparent at longer incubation times. The incubations with *Ac*Xyn10A resulted in a more abundant production of xylose (X_1) and xylobiose (X_2) and smaller decorated oligosaccharides (i.e. A^3X) compared to *Tl*Xyn11 (Fig. 3c-d), as expected from the substrate tolerance of family GH10 xylanases.

In contrast, the *B*Xyn8 produced much longer products, mostly linear XOS of up to a xylopentaose (X_1-X_5) (Fig. 3e). *B*Xyn8 had initially produced xylohexaose (X_6) after 1 to 3 h of hydrolysis, but it was further hydrolysed after 48 h (Fig. 3f). Other GH8 xylanases reported in literature have produced XOS with up to 3–5 units, depending on the organism (Pollet, Schoepe, et al., 2010; Ray et al., 2019), which suggests high variability of this family of enzyme. The *B*Xyn8 also produced substituted (A)XOS, predominantly XA^3XX followed by XA^2XX and $A^{2,3}XX$, in which the latter was largely depleted after 48 h (Fig. 3f, ESI Fig. S6e). In RAX, XA^3XX was one of the most abundant products released, reflecting both the highly substituted nature of RAX but also the tight spacing of the Ara*f* substitutions, where low amounts of long linear XOS were produced in comparison to WAX.

HPAEC-PAD analysis of the hydrolysates from *Gp*Xyn5_34 revealed very distinct profiles compared to the other xylanases (Fig. 3g). Firstly, many more chromatographic peaks were present, of which only some could be putatively assigned to standards. *Gp*Xyn5_34 produced both linear and substituted oligosaccharides (Fig. 3h, ESI Fig. S6g and S6h), whereby XA^3XX was the most abundant, especially in RAX. This result is in agreement with Bhattacharya et al. (2020), who studied the hydrolysis products of a GH5_34 xylanase from *C. thermocellum* on wheat AX. Interestingly, *Gp*Xyn5_34 did not further degrade the released oligosaccharides, as absence of a C(O)-3 linked Ara*f* in the released oligosaccharides likely prevented further degradation. Secondly, the signal of (A)XOS observed on the HPEAC-PAD profiles was particularly low, even in RAX (Fig. 3g, ESI Fig. S6g) whereby the amount of reducing sugar was higher than that of *B*Xyn8 and *Tl*Xyn11 (Fig. 2a). This implied that the hydrolysis products released by *Gp*Xyn5_34 were longer than the maximum size detectable by HPAEC-PAD, which highlighted the need of other methods to analyse the hydrolysate.

3.1.3. *Structural elucidation of unidentified (A)XOS using LC-MS²*

To elucidate the structure of (A)XOS that do not correspond to available standards in the HPAEC-PAD, the hydrolysate of Rb FAX was chemically labelled with reduction/per-methylation and analysed by LC-ESI-MS^2. With the LC-ESI-MS^2 analysis, we aimed to provide further insights into where Ara*f* substitution was tolerated, especially for *B*Xyn8 and *Gp*Xyn5_34. By selecting the ions 565 *m/z* and 725 m/z that corresponded to P3 (3-unit pentose) and P4 ions respectively, we resolved and identified 12 different (A)XOS structures from the different hydrolysates (Fig. 4a and ESI Fig. S7), 8 of which could not be observed in the HPEAC-PAD. In the P3 (565 m/z) chromatograms, peak 1 and 3 were identified from labelled standards, while peak 2 that corresponded to XA^3, was determined from the fragmentation spectra (Fig. S7a). The prevalence of peak 2 (XA^3) in the hydrolysate of *Gp*Xyn5_34 confirmed the tendency of *Gp*Xyn5_34 to produce (A)XOS with a C(O)3-linked Ara*f* on the reducing end (Correia et al., 2011; Labourel et al., 2016). Meanwhile for *Tl*Xyn11 and *B*Xyn8, the Ara*f* on XA^3 would likely be tolerated at the +2 subsite (Pollet et al., 2009; Pollet, Schoepe, et al., 2010).

In the P4 (725 *m/z*) chromatograms, both the *Tl*Xyn11 and *B*Xyn8 produced large peaks corresponding to a linear X_4 (peak 5) and XA^3X

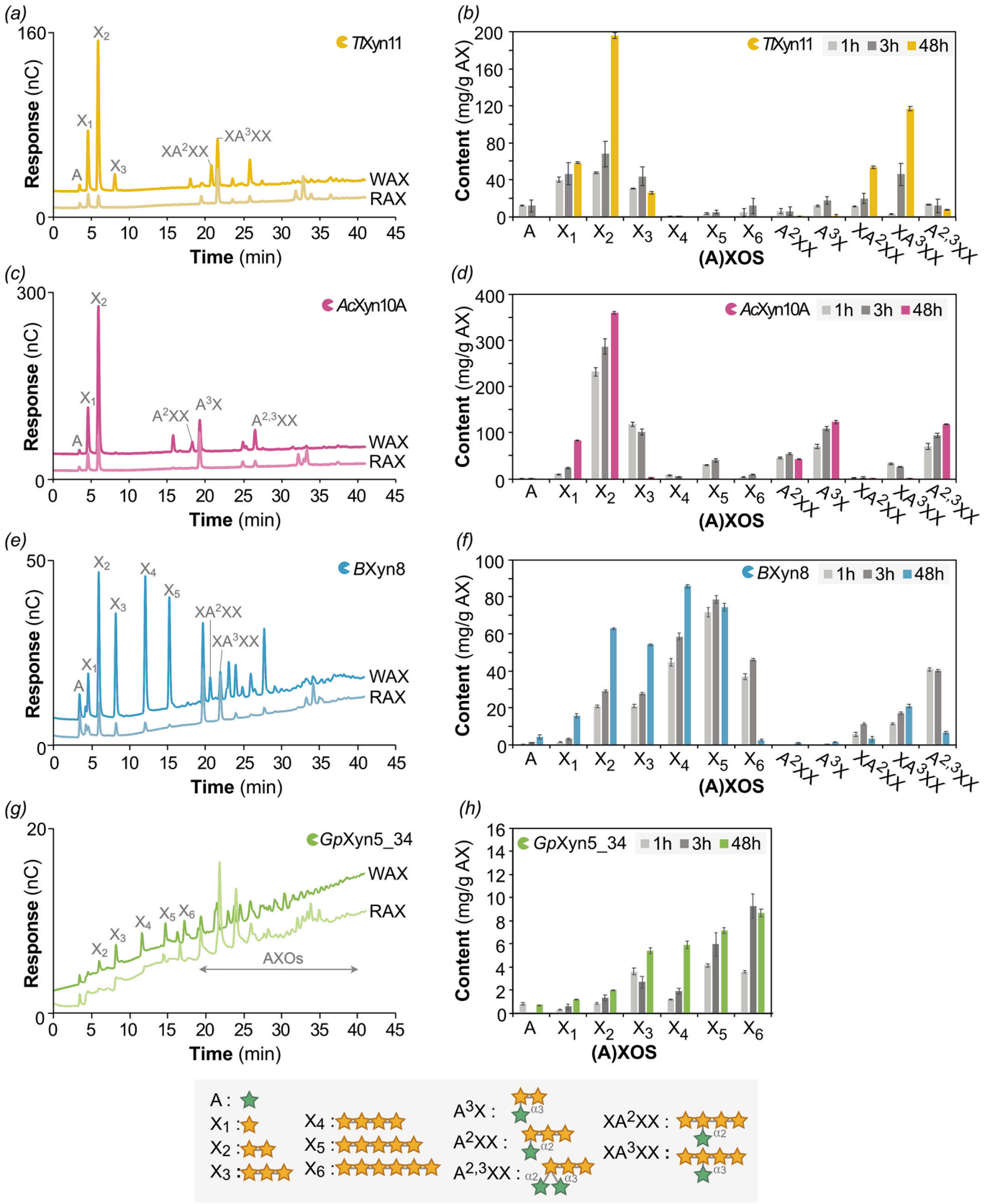

Fig. 3. HPAEC-PAD profiles of oligosaccharides from the hydrolysis of WAX and RAX. (a, c, e, f) HPAEC-PAD profiles of enzymatic hydrolysates on WAX and RAX after 48 h. Quantified (A)XOS from the hydrolysis of WAX in reference to available standards after 1 h, 3 h and 48 h of incubation for (b) *Tl*Xyn11, (d) *Ac*Xyn10A, (f) *B*Xyn8 and (h) *Gp*Xyn5_34. Error bars show deviation of triplicate analysis.

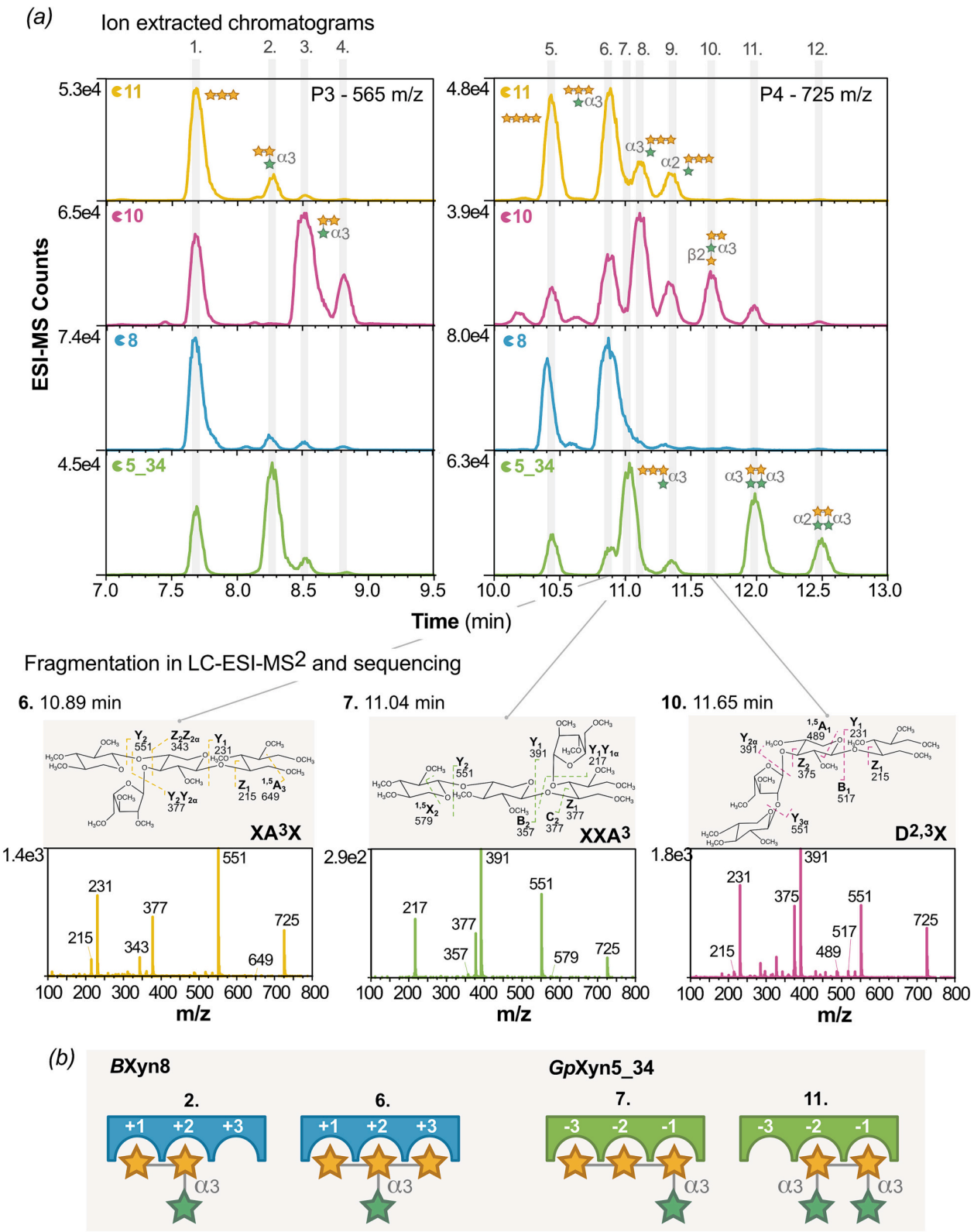

Fig. 4. Oligosaccharide profiling of arabinoxylan-oligosaccharides using LC-ESI-MS^2. (a) Single ion monitoring (SIM) chromatogram of arabinoxylan oligosaccharides from Rb FAX after xylanase hydrolysis and reduction/per-methylation. Mass spectra (MS^2) of selected peaks from SIM shown in terms of sodiated adducts $[M + Na]^+$ and proposed sequencing of oligosaccharide structure. Note: P (pentose, could either be Xyl*p* or Ara*f*). Fragmentation and proposed assignation of peaks not mentioned in the figure is presented in ESI Fig. S7 (Domon & Costello, 1988). The sequenced oligosaccharide structures are named following the systematic nomenclature for xylo-oligosaccharides proposed by Fauré et al. (2009). (b) Proposed subsite tolerance for arabinose substitution from selected (A)XOS by *B*Xyn8 and *Gp*Xyn5_34.

(peak 6). The presence of XA^3X in the hydrolysate of *Tl*Xyn11 was expected. However, for *B*Xyn8 this result supported that Ara*f* was likely tolerated at the +2 subsite (Fig. 4b), as substitutions are less tolerated in the glycone region (subsites −3 and −2) (Pollet, Schoepe, et al., 2010; Vos et al., 2006). The fact that no other structures were prevalent in the hydrolysate of *B*Xyn8 also implied that subsite +1 could not accommodate substitution. Furthermore, in the hydrolysate of *Ac*Xyn10A, the oligosaccharide $D^{2,3}X$ was proposed for peak 10 (Juvonen et al., 2019). It is reported that the −2 subsite of GH10 xylanases can accommodate large substitutions such as ferulic acid-Ara*f* (Vardakou et al., 2005), thus making it plausible that a $D^{2,3}$ motif can also be accommodated at this subsite (Juvonen et al., 2019).

In the hydrolysate of *Gp*Xyn5_34, 3 peaks corresponding to P4 dominated the chromatogram i.e., peak 7, 11 and 12. Interestingly, peak 7 that corresponded to XXA^3, was only observed with *Gp*Xyn5_34, further signifying that only the GH5_34 xylanase could tolerate (or require) Ara*f* substitution at the −1 subsite (Fig. 4b). Peak 11 and 12 also corresponded to AXOS having an Ara*f* at the reducing end, with another Ara*f* at the non-reducing end. This additionally confirmed that the *Gp*Xyn5_34 could tolerate Ara*f* at the −2 subsite, which is in agreement with literature (Labourel et al., 2016). In the fragmentation spectra, Ara*f* substitution at the reducing end was determined from the diagnostic ion of 217 *m/z*, which appeared on the spectra of XA^3, XXA^3, A^3A^3 and A^2A^3 but not on all the other spectra. The possibility for a double substitution to be sitting on the reducing was also ruled out as it would have resulted in an ion that was smaller than 217 m/z, which was not observed in any of the spectra. This indicates the capability of *Gp*Xyn5_34 at cleaving in highly substituted areas of cereal AX with consecutive arabinose decorations, which are inaccessible for other xylanase families.

3.2. Exploration of the distribution of arabinose and ferulic acid substitutions along the AX backbone

3.2.1. Occurrence of long arabinoxylan-oligosaccharides

To study the presence of longer oligosaccharides, we performed oligosaccharide mass profiling (OLIMP) on the hydrolysis products after 48 h. The OLIMP does not provide explicit information about the structure of the oligosaccharides as it does not discriminate the isobaric nature of pentoses (Xyl*p* and Ara*f*). The OLIMP profiles from the hydrolysis of RAX (ESI Fig. S9a) revealed that much longer oligosaccharides of up to 14 pentose units (P14) were indeed present in the hydrolysates. Among the OLIMP profiles from the hydrolysis of WAX, RAX and Rb F-AX (ESI Fig. S8a, ESI Fig. S9a and Fig. 5a), *Ac*Xyn10A produced the narrowest range (up to P10 in RAX), while *Gp*Xyn5_34 produced the widest range (up to P14 in RAX).

We investigated the length of the oligosaccharides in more detail by removing the arabinose substitution on the (A)XOS after xylanase treatments using *Mg*Abf51 and *Hi*Abf43_36, which are arabinofuranosidases that cleave single Ara*f* substitutions and the C(O)-3 linked Ara*f* from a double substitution, respectively (McKee et al., 2012; Sorensen et al., 2007). The resulting arabinose-free XOS backbones were then subjected to another OLIMP analysis (Fig. 5 and ESI Fig. S8b, ESI Fig. S9b). Interestingly, in RAX both *Gp*Xyn5_34 and *B*yn8 produced the longest XOS backbones of up to P11 (11 xylose units). In the long hydrolysates of *B*yn8, several arabinose substitutions could have been present in the (A)XOS, thus preventing it from being further hydrolysed. In contrast, the products released by *Gp*Xyn5_34 are not further degraded and thus the OLIMP of the XOS backbones suggests that the C(O)3 Ara*f* can be spaced 11 xylose units apart. Meanwhile, the backbones produced by *Ac*Xyn10A and *Tl*Xyn11 are generally shorter, reaching P7 in RAX.

3.2.2. All xylanases generate feruloylated arabinoxylan-oligosaccharides (F-AXOS) from Rb F-AX

Some of the (A)XOS produced from the hydrolysis of Rb F-AX were expected to contain ferulic acid (FA), as Rb F-AX contained 8.9 mg/g of FA. The amount of FA is not substantial (approximately one FA every 75 xylose units, taking into account the purity of the Rb F-AX); however, its low presence can still contribute to antioxidant properties and modulation of the gut microbiota when consumed as part of a prebiotic (Castelluccio et al., 1996; Snelders et al., 2014). Indeed, ferulic acid can be metabolised by some bacterial species (i.e. Bacteroides species) and generate metabolites such as vinyl phenol derivatives or phenyl propionic acids (Pereira et al., 2021; Snelders et al., 2014). In the OLIMP profiles of the Rb F-AX hydrolysate (Fig. 5a), F-AXOS composed of up to 7 pentose units (P7F) were present in the hydrolysates. This highlighted that FA-Ara*f* substitutions could be accommodated by all the enzymes. It has been reported that the GH10 xylanase can accommodate FA-Ara*f* at subsite −2 (Vardakou et al., 2005), while the GH11 xylanase can accommodate it at subsite +2 (Vardakou, Dumon, et al., 2008). However, the position at which FA-Ara*f* can be accommodated for GH5 and GH8 xylanases has not been reported before. Interestingly, after arabinose removal by *Mg*Abf51 and *Hi*Abf43_36, the majority of the F-AXOS profiles remained the same (Fig. 5b), indicating that presence of FA likely hindered the activity of the arabinofuranosidases, which is in agreement with previous studies (Luonteri et al., 1999; Rémond et al., 2008). Our study showed for the first time that both GH5 and GH8 xylanases can tolerate the presence of FA in the substrate and release feruloylated oligosaccharides (F-AXOS), although the exact positioning in the enzyme active site requires further attention.

3.2.3. Presence of partially digested oligo- and polysaccharide populations

To determine the presence of partially or undigested polysaccharides, size exclusion chromatography (SEC) was performed on the 48 h hydrolysates. The SEC results revealed that indeed both oligosaccharides and polysaccharides were present in the hydrolysates, depending on the type of substrate (Fig. 5c-5e). Interestingly, all the WAX hydrolysates were largely unimodal (Fig. 5c), ranging progressively from small polysaccharides (between 10^3 and 10^4 Da) for *Gp*Xyn5_34 to small oligosaccharides for *Ac*Xyn10A. The unimodal distribution of hydrolysis products for all the enzymes suggests that the Ara*f* substitutions were somewhat steadily distributed throughout the backbone. Indeed, a levelled spacing of Ara*f* throughout the polymeric backbone would allow for those that were sterically hindered by substitution, (*Tl*Xyn11 and *B*yn8) and the *Gp*Xyn5_34, which required substitution, to cleave the WAX at specific sites throughout the polysaccharide.

On the other hand, the RAX hydrolysate (Fig. 5d) displayed several distinct populations corresponding to small oligosaccharides and polysaccharides. A clear peak at 10^3 Da was observed and likely corresponded to oligosaccharides, which was clearly present in the hydrolysate of *Tl*Xyn11, *Ac*Xyn10A and *Gp*Xyn5_34. Meanwhile, *B*yn8 displayed its highest distribution at 10^3–10^4 Da, confirming that it could not effectively cleave the highly substituted RAX substrate. Interestingly, a peak between 10^4 and 10^5 Da was present in all the hydrolysates, while another peak between 10^5 and 10^6 Da was only present in the hydrolysate of *Tl*Xyn11 and *B*yn8. This suggests the presence of AX populations containing blocks of heavily substituted regions, which are inaccessible for *Tl*Xyn11 and *B*yn8 but could be cleaved by *Ac*Xyn10A and *Gp*Xyn5_34, and other blocks of largely unsubstituted backbones that could not be cleaved by *Gp*Xyn5_34. This evidences the occurrence of complex intramolecular domains with distinct substitution patterns in the xylans from cereal cell walls (Saulnier et al., 2007; Viëtor et al., 1994), which may influence the interaction with other cell wall components (Tryfona et al., 2023).

Lastly, in the hydrolysate of Rb F-AX (Fig. 5e), three evident distributions were present centred at 10^3, 10^4, and 10^5 Da, respectively. For the hydrolysate of *Tl*Xyn11 and *Ac*Xyn10A, all three distributions were present; in *B*yn8, only the distributions at 10^3 and 10^4 Da were present, while in *Gp*Xyn5_34, the population at 10^4 Da was absent but a population at 10^5 Da was clearly present. The latter could refer to linear populations with very low Ara*f* substitution that were perhaps

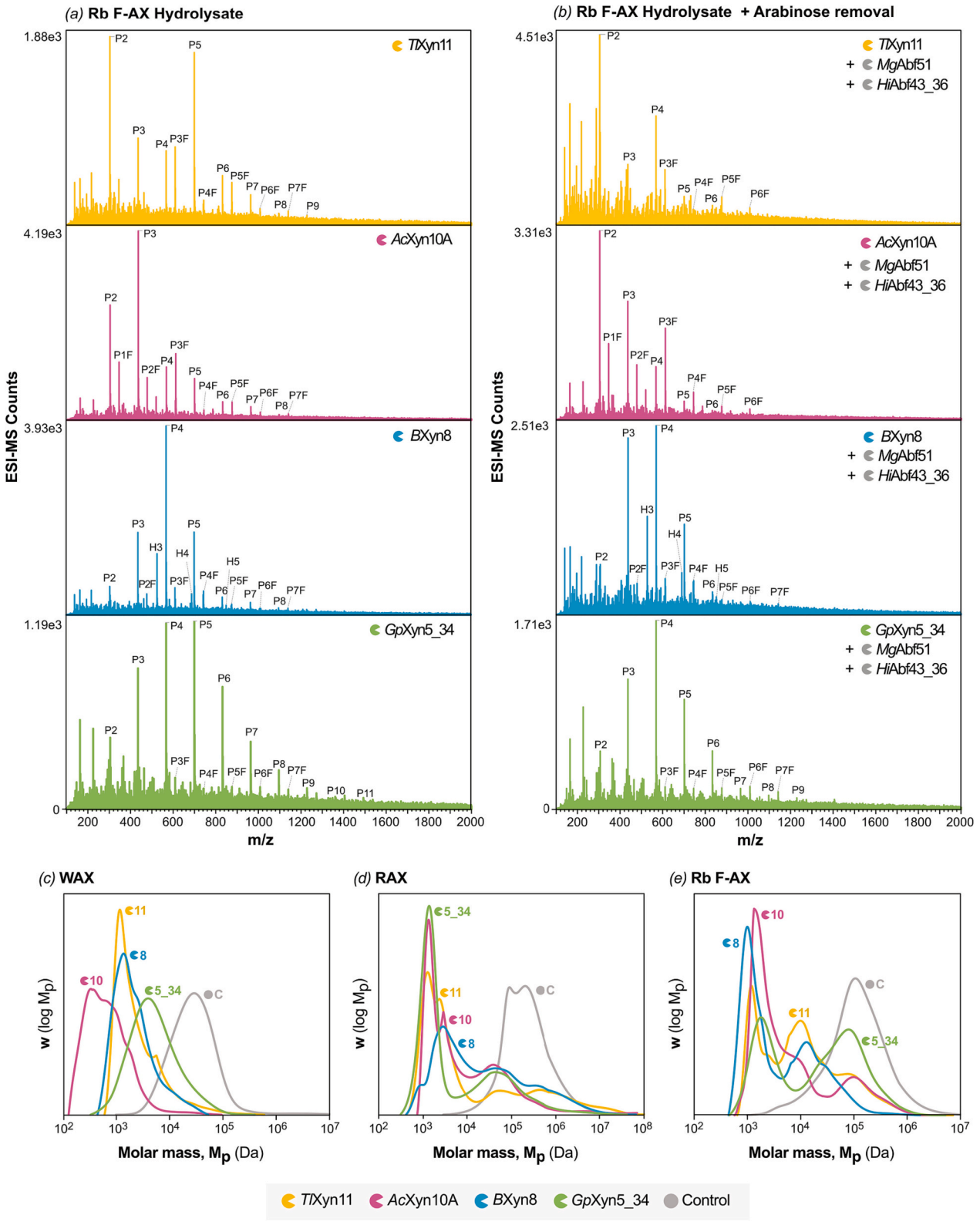

Fig. 5. Characterisation of longer oligosaccharide and polysaccharide products. (a) Oligosaccharide mass profiling (OLIMP) of Rb F-AX hydrolysate after xylanases treatment for 48 h. (b) OLIMP of Rb F-AX hydrolysate after 48 h with xylanases followed by arabinose removal by *Mg*Abf51 and *Hi*Abf43_36. Mass profiling was performed using ESI-MS and the spectra is shown in terms of the mass to charge ratios (m/z) of sodiated adducts $[M + Na]^+$. Note P: pentose, H: hexose and F: ferulic acid. Molar mass distributions of arabinoxylans with and without xylanase treatment from (c) WAX, (d) RAX and (e) Rb F-AX. Samples were analysed using SEC in DMSO/LiBr using a calibration of linear pullulan standards.

uncleavable by the *Gp*Xyn5_34. The peak at 10^5 Da could also be attributed to mixed-linked β-glucans that was present as a minor population in the Rb FAX extract (ESI Table S2). Interestingly this peak was absent in the profile of *B*yn8, implying that this enzyme exhibited a side activity towards mixed-linked β-glucans, as we confirmed in ESI Fig. S4.

3.2.4. *Models for the distribution of arabinose substitutions in cereal AXs*

As confirmed in this study, the *Gp*Xyn5_34 specifically cleaved after a C(O)-3 linked Ara*f*. This exceptional trait was further explored to understand how single C(O)-3 linked Ara*f*s were spaced out on the AX substrates. An approximation of the Ara*f* distributions based on the SEC, OLIMP, HPEAC-PAD and glycosidic linkage data is shown in Fig. 6, where a detailed summary of how the figures were proposed can be found in Supplementary method 8, ESI Table S4 and ESI Table S5. Among the AX substrates, WAX was the only one that displayed a unimodal SEC distribution after hydrolysis (Fig. 5c). This suggests that Ara*f* substitutions in WAX are steadily distributed and that there is likely only one dominating population present. Meanwhile, the OLIMP profile from the hydrolysate of *Gp*Xyn5_34 (ESI Fig. S8b) revealed that the xylopyranosyl backbones of the (A)XOS released from WAX ranged between 2 and 11 units, whereby the 4-unit xylotetraose was most prevalent. Considering the specificity of the *Gp*Xyn5_34, the length of the xylopyranosyl backbones likely indicates the spacing of the C(O)-3 linked Ara*f*s. The spacing of the C(O)-2 and C(O)-2,3 linked Ara*f*s, however, could not be determined (Fig. 6a).

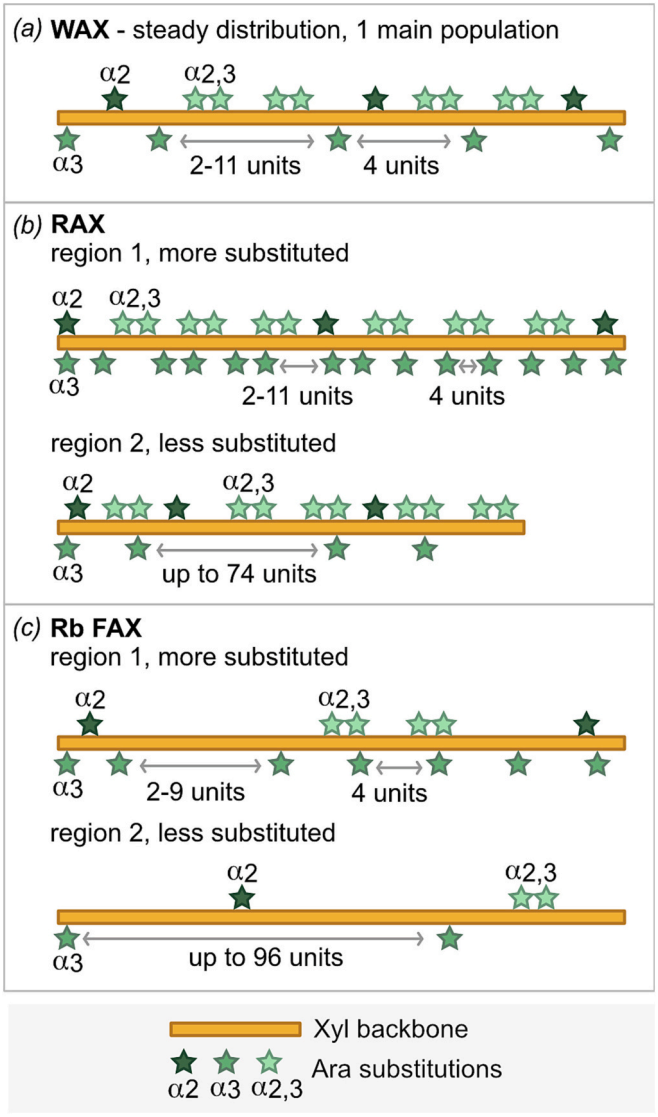

Fig. 6. Approximation of the arabinose distribution on the arabinoxylan substrates based on the product profiles after enzymatic hydrolysis. (a) WAX is composed of one main population, displaying a steady distribution of arabinoses. (b) RAX is composed of two regions, where region one is more substituted than the other. Region one is more prevalent than region two. (c) Rb FAX is also composed of two regions where one is more substituted than the other.

In the case of RAX and Rb FAX, a bimodal distribution was observed in the SEC profiles after *Gp*Xyn5_34 hydrolysis (Fig. 5d and e), which suggested that there are likely two regions present, whereby one is more substituted than the other. In the SEC profile of *Gp*Xyn5_34 in RAX (Fig. 5d), an uneven distribution was observed between the low molar mass peak (region 1, high substitution) and the higher molar mass peak (region 2, low substitution), inferring that region 1 was longer than region 2 (Fig. 6b). In region 1 of RAX, a similar distribution of the C(O)-3 linked Ara*f*s was observed to that of WAX, which was determined based on the OLIMP data (ESI Fig. S9b). For region 2 of RAX, the C(O)-3 linked Ara*f* was approximated to be spaced apart by 74 units, while the other Ara*f* motifs likely remained in close proximity, as supported by the low amount of long linear XOS produced by *B*Xyn8 (Fig. 3e). In Rb FAX, as less Ara*f* was present, distribution was approximated to reach a spacing of up to 96 units in region 2. The proposed models only give an initial indication of how specific Ara*f*s could be distributed on the AXs. The model has its limitations, including the overgeneralisation of one monosaccharide data to represent two different regions with differing degrees of substitutions. Nonetheless, this approach highlights the key importance of using highly specific GH5 xylanases to understand complex AX structures.

3.3. *The profile of (A)XOS influences the growth and metabolite production by gut bacteria in vitro*

To investigate the implication of different (A)XOS profiles in terms of their prebiotic potential, in vitro fermentation was performed on *Bacteroides ovatus*, which is regarded as a polysaccharide degrader (Rogowski et al., 2015; Smith et al., 2006) and *Bifidobacteria adolescentis*, which is a targeted probiotic that contributes to gut homeostasis (Falck et al., 2013; Riviere et al., 2016). The chosen substrates were the WAX hydrolysates, as all the enzymes were moderately active on WAX and the hydrolysates showed the greatest difference in structure among the different enzymes. The choice for WAX also meant that feruloylated AX was not investigated in terms of their prebiotic effect in this study.

Hydrolysis of WAX into (A)XOS substantially increased the growth of *B. ovatus*, as this bacterium was unable to grow on polymeric WAX i.e., in the control and hydrolysate of *Gp*Xyn5_34 (Fig. 7a). Maximum growth of *B. ovatus* was achieved in the hydrolysates of *B*Xyn8 and *Tl*Xyn11, while in the hydrolysate of *Ac*Xyn10A, growth was moderate. It appeared that the *B. ovatus* could not directly use polymeric AX as its main carbon source, neither did it consume the X_2-rich hydrolysate of the *Ac*Xyn10A. In the hydrolysate of *Tl*Xyn11 and *B*Xyn8, the amounts and variety of small and larger (A)XOS was more diverse, providing a wider range of carbon sources for the bacteria. During fermentation on the *Tl*Xyn11 hydrolysate, *B. ovatus* consumed mostly X_2 and X_3 but also XA^2XX and XA^3XX, while X_1 accumulated from 8 h onwards (Fig. 7c). In the *B*Xyn8 hydrolysate, X_4 and X_5 were initially consumed while X_2 and X_3 increased until 24 h and 8 h, respectively. Arabinose also accumulated after 24 h and was then consumed together with the majority of linear X_1 to X_5 at 48 h. In agreement with the high growth in the hydrolysates of *Tl*Xyn11 and *B*Xyn8, notable amounts of short chain fatty acids (SCFA) were produced in these cultivations. Propionate remained constant throughout the fermentation period, while acetate increased over time (Fig. 7g). The delicate preference of *B. ovatus* to utilise specific (A)XOS, i.e. longer linear XOS, over monomeric xylose or polymeric AX, was likely governed by their membrane-bound multi-protein degrading

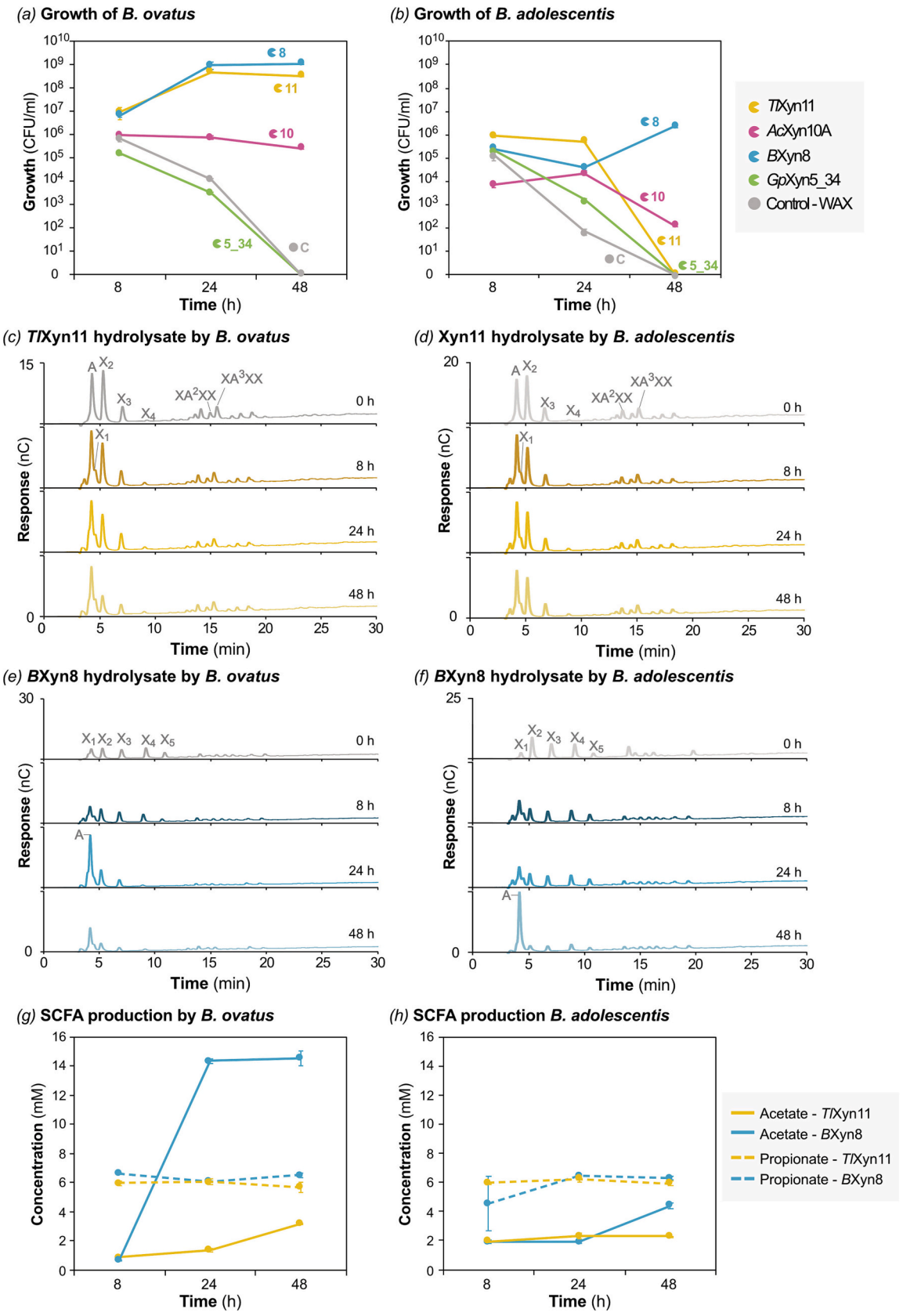

Fig. 7. In vitro fermentation of (A)XOS by gut bacteria. Growth of (a) *B. ovatus* and (b) *B. adolescentis* on WAX hydrolysates. Utilisation of (A)XOS during fermentation from the hydrolysates of (c,d) *Tl*Xyn11 and (e, f) *B*Xyn8 after 0 h, 8 h, 24 h and 48 h. Short chain fatty acid (SCFA) production from the cultivation of *(g) B. ovatus* and *(h) B. adolescentis*.

systems, coordinated by several polysaccharide utilisation loci in their genome (Pereira et al., 2021; Rogowski et al., 2015). These complex systems are induced by specific substrates and are otherwise repressed by readily available sugars (Grondin et al., 2017; Martens et al., 2009; Smith et al., 2006). Such highly regulated systems could explain the reluctance for the *B. ovatus* to utilise the X_2-rich hydrolysate of *Ac*Xyn10A, considering that in the hydrolysates of *Tl*Xyn11 and *B*Xyn8, X_2 was consumed together and/or after consumption of more complex X_3, X_4, X_5, XA^2XX and XA^3XX.

For *B. adolescentis*, a similar preference was observed towards the hydrolysates of *Tl*Xyn11 and *B*Xyn8, although after 24 h only the hydrolysate of *B*Xyn8 could promote further growth of the bacteria (Fig. 7b). *B. adolescentis* could utilise the hydrolysate of *Ac*Xyn10A until 48 h, however, the growth steadily declined. As for the hydrolysate of *Gp*Xyn5_34 and the undigested WAX, *B. adolescentis* could not use these carbon sources likely because it is not known to produce xylanases (Riviere et al., 2016). During fermentation of the *Tl*Xyn11 hydrolysate, X_2 was slightly consumed after 8 h, while in the hydrolysate of *B*Xyn8, X_2 to X_5 were gradually consumed throughout the fermentation period (Fig. 7d and f). Interestingly after 48 h, *B. adolescentis* accumulated arabinose, inferring that after release of the substitution, it only consumed the linear XOS backbone, which was previously observed by Pastell et al. (2009). It has also been reported that *B. adolescentis* produces a reducing-end xylose-releasing exo-oligoxylanase from GH8 that acts upon XOS substrates with a DP of >2, further supporting its preference for longer XOS (Lagaert et al., 2007). The promoted growth on the *B*Xyn8 hydrolysate consequently led to a higher production of acetate, whilst propionate remained constant throughout the fermentation (Fig. 7h). Other metabolites such as succinate and lactate were also produced during fermentation, as shown ESI Fig. S12.

Preference towards specific (A)XOS is observed at species level, whereby the hydrolysis and/or metabolic products released become potential substrates for other bacterial species co-habiting the gut (Crittenden et al., 2002). This highlights that the results shown in this study only illustrate a glimpse on the complexity of bacterial utilisation and cross-feeding interactions that occur in vivo. Nevertheless, the results have highlighted that key oligosaccharide structures, i.e. longer linear XOS, were much more readily consumed by both *B. ovatus* and *B. adolescentis*, resulting in higher growth and subsequent production of short chain fatty acids. From a substrate perspective, we can also extrapolate that the use of Rb F-AX, with a lower degree of arabinose substitution, would result in the production of a higher abundance of longer linear XOS (ESI Fig. S6), which would in principle promote the growth and functionality of *B. ovatus* and *B. adolescentis*. However, the effect of the ferulic acid still needs to be evaluated.

4. Conclusions

In this study, we have compared the activity of less characterised xylanases from GH8 (*B*Xyn8) and GH5_34 (*Gp*Xyn5_34) with those that are well-known from GH10 (*Ac*Xyn10A) and GH11 (*Tl*Xyn11) on arabinoxylans (AX) substrates with differing substitution patterns. The *Ac*Xyn10A and *Tl*Xyn11 exhibited higher hydrolytic activity on the AX substrates and produced small hydrolysis products (mainly X_2), while the *B*Xyn8 produced longer linear xylooligosaccharides (XOS) of up to X_5. The *B*Xyn8 was most hindered by arabinose (Ara*f*) substitution but could still accommodate them at the +2 subsite, while the *Gp*Xyn5_34 preferred highly substituted AX, requiring an Ara*f* at the −1 subsite for cleavage. The *Gp*Xyn5_34 produced arabinoxylan-oligosaccharides or (A)XOS that was substituted at the reducing end. It is well known that enzymatic loading affects the product profiles after hydrolysis, but this should be the subject for further investigation. On the hydrolysis of rye bran feruloylated-arabinoxylan (Rb F-AX), all the xylanases could release (A)XOS bearing a ferulic acid (FA), although the exact binding of the ferulic acid in the enzyme active site still requires further investigation. The unique specificity *Gp*Xyn5_34 also provided an initial insight into how Ara*f* distributions differed among the AX substrates. Wheat endosperm AX (WAX) with moderate A/X ratio exhibited a regular distribution of Ara*f* substitutions, whereas highly substituted rye endosperm AX (RAX) and rye bran AX (Rb-F-AX) display two separate regions with distinct distribution of substitutions. It is worth mentioning that the reported xylanases have been selected based on their reported canonical specificity, but the results cannot be extrapolated to all the xylanases from the studied families. Further study on the prebiotic potential of the (A)XOS revealed that the hydrolysate of *B*Xyn8 rich in linear XOS promoted the best growth of *Bacteroides ovatus* and *Bifidobacterium adolescentis*, along with the highest production of acetate. We show that the combination of the applied cereal AX substrate and xylanase family determines the production of oligosaccharides and their molecular structure, which in turn influence their utilisation by selected gut bacteria and the production of beneficial metabolites such as short chain fatty acids. The presence of feruloylation in the AX substrate is likely to impact both its deconstruction by the different enzyme families into feruloylated AXOS and their fermentability by gut bacteria. This study has large implications for the potential incorporation of arabinoxylan oligosaccharides in food and feed products with high dietary fibre content and potential prebiotic activities, resulting in improved host health.

CRediT authorship contribution statement

Reskandi C. Rudjito: Investigation, Methodology, Formal analysis, Writing – original draft. **Amparo Jiménez-Quero:** Investigation, Methodology, Supervision, Writing – review & editing. **Maria Del Carmen Casado Muñoz:** Investigation, Methodology. **Teun Kuil:** Investigation, Writing – review & editing. **Lisbeth Olsson:** Conceptualization, Writing – review & editing. **Mary Ann Stringer:** Investigation, Resources, Writing – review & editing. **Kristian Bertel Rømer Mørkeberg Krogh:** Conceptualization, Resources, Writing – review & editing. **Jens Eklöf:** Conceptualization, Resources, Writing – review & editing. **Francisco Vilaplana:** Conceptualization, Supervision, Funding acquisition, Project administration, Writing – review & editing.

Declaration of competing interest

The authors declare the following financial interests/personal relationships which may be considered as potential competing interests: Francisco Vilaplana reports financial support was provided by Swedish Research Council Formas. Francisco Vilaplana reports financial support was provided by Lantmännen Research Foundation. Francisco Vilaplana reports a relationship with Oatly AB that includes: employment. Mary Ann STRINGER reports a relationship with Novozymes Inc. that includes: employment. Kristian Bertel Romer Morkeberg KROGH reports a relationship with Novozymes Inc. that includes: employment. Jens EKLOF reports a relationship with Novozymes Inc. that includes: employment. None.

Data availability

Data will be made available on request.

Acknowledgements

This work was funded by the Swedish Research Council FORMAS (Project 942-2016-119) and the Lantmännen Research Foundation (Project 2016F008). FV and LO acknowledge the Wallenberg Wood Science Centre (WWSC) funded by the Knut and Alice Wallenberg Foundation for the support building up the analytical capabilities used in this work. We would also like to acknowledge Dr. Annelie Moldin (Lantmännen) and Dr. Andrés Jesus Rascón Lopez (Royal Institute of Technology) for valuable discussions.

Appendix A. Supplementary data

Supplementary data to this article can be found online at https://doi.org/10.1016/j.carbpol.2023.121233.

References

AACC. (2001). The definition of dietary fiber. *Cereal Foods World, 46*(3), 112–126.

Aftab, U., & Bedford, M. R. (2018). The use of NSP enzymes in poultry nutrition: Myths and realities. *World's Poultry Science Journal, 74*(2), 277–286.

Bhattacharya, A., Ruthes, A., Vilaplana, F., Karlsson, E. N., Adlecreutz, P., & Stålbrand, H. (2020). Enzyme synergy for the production of arabinoxylo-oligosaccharides from highly substituted arabinoxylan and evaluation of their prebiotic potential. *Food Science and Technology, 131*, Article 109762.

Biely, P., Vršanská, M., Tenkanen, M., & Kluepfel, D. (1997). Endo-β-1,4-xylanase families: Differences in catalytic properties. *Journal of Biotechnology, 57*(1–3), 151–166.

Broekaert, W., Courtin, C., Verbeke, K., Van De Wiele, T., Verstraete, W., & Delcour, J. (2011). Prebiotic and other health-related effects of cereal-derived arabinoxylans, arabinoxylan-oligosaccharides, and xylooligosaccharides. *Critical Reviews in Food Science and Nutrition, 51*(2), 178–194.

Castelluccio, C., Bolwell, G. P., Gerrish, C., & Rice-Evans, C. (1996). Differential distribution of ferulic acid to the major plasma constituents in relation to its potential as an antioxidant. *The Biochemical Journal, 316*(Pt 2), 691–694.

Chen, H., Wang, W., Degroote, J., Possemiers, S., Chen, D., De Smet, S., & Michiels, J. (2015). Arabinoxylan in wheat is more responsible than cellulose for promoting intestinal barrier function in weaned male piglets. *The Journal of Nutrition, 145*(1), 51–58.

Chen, Z., Li, S., Fu, Y., Li, C., Chen, D., & Chen, H. (2019). Arabinoxylan structural characteristics, interaction with gut microbiota and potential health functions. *Journal of Functional Foods, 54*, 536–551.

Collins, T., Gerday, C., & Feller, G. (2005). Xylanases, xylanase families and extremophilic xylanases. *FEMS Microbiology Reviews, 29*(1), 3–23.

Correia, M. A. S., Mazumder, K., Brás, J. L. A., Firbank, S. J., Zhu, Y., Lewis, R. J., … Gilbert, H. J. (2011). Structure and function of an arabinoxylan-specific xylanase. *The Journal of Biological Chemistry, 286*(25), 22510–22520.

Crittenden, R., Karppinen, S., Ojanen, S., Tenkanen, M., Fagerström, R., Mättö, J., … Poutanen, K. (2002). In vitro fermentation of cereal dietary fibre carbohydrates by probiotic and intestinal bacteria. *Journal of the Science of Food and Agriculture, 82*(8), 781–789.

Delzenne, N. M., Cani, P. D., Everard, A., Neyrinck, A. M., & Bindels, L. B. (2015). Gut microorganisms as promising targets for the management of type 2 diabetes. *Diabetologia, 58*(10), 2206–2217.

Demuth, T., Edwards, V., Bircher, L., Lacroix, C., Nyström, L., & Geirnaert, A. (2021). In vitro colon fermentation of soluble arabinoxylan is modified through milling and extrusion. *Frontiers in Nutrition, 8*.

Diether, N., & Willing, B. (2019). Microbial fermentation of dietary protein: An important factor in diet–microbe–host interaction. *Microorganisms, 7*(1), 19.

Domon, B., & Costello, C. E. (1988). A systematic nomenclature for carbohydrate fragmentations in FAB-MS/MS spectra of glycoconjugates. *Glycoconjugate Journal, 5*(4), 397–409.

Ebringerová, A., & Heinze, T. (2000). Xylan and xylan derivatives – Biopolymers with valuable properties, 1. Naturally occurring xylans structures, isolation procedures and properties. *Macromolecular Rapid Communications, 21*(9), 542–556.

EFSA Panel on Dietetic Products, N. a. A. (2010). Scientific opinion on dietary reference values for carbohydrates and dietary fibre. *EFSA Journal, 8*(3), n/a.

Falck, P., Aronsson, A., Grey, C., Stålbrand, H., Nordberg Karlsson, E., & Adlercreutz, P. (2014). Production of arabinoxylan-oligosaccharide mixtures of varying composition from rye bran by a combination of process conditions and type of xylanase. *Bioresource Technology, 174*, 118–125.

Falck, P., Linares-Pastén, J. A., Karlsson, E. N., & Adlercreutz, P. (2018). Arabinoxylanase from glycoside hydrolase family 5 is a selective enzyme for production of specific arabinoxylooligosaccharides. *Food Chemistry, 242*, 579–584.

Falck, P., Precha-Atsawanan, S., Grey, C., Immerzeel, P., Stålbrand, H., Adlercreutz, P., & Nordberg Karlsson, E. (2013). Xylooligosaccharides from hardwood and cereal xylans produced by a thermostable xylanase as carbon sources for Lactobacillus brevis and Bifidobacterium adolescentis. *Journal of Agricultural and Food Chemistry, 61*(30), 7333–7340.

Fauré, R., Courtin, C. M., Delcour, J. A., Dumon, C., Faulds, C. B., Fincher, G. B., … O'Donohue, M. J. (2009). A brief and informationally rich naming system for oligosaccharide motifs of heteroxylans found in plant cell walls. *Australian Journal of Chemistry, 62*, 533–537.

Fujimoto, Z., Kaneko, S., Kuno, A., Kobayashi, H., Kusakabe, I., & Mizuno, H. (2004). Crystal structures of decorated xylooligosaccharides bound to a family 10 xylanase from Streptomyces olivaceoviridis E-86. *The Journal of Biological Chemistry, 279*(10), 9606–9614.

Gallardo, C., Jiménez, L., & García-Conesa, M. T. (2006). Hydroxycinnamic acid composition and in vitro antioxidant activity of selected grain fractions. *Food Chemistry, 99*(3), 455–463.

Gibson, G. R., Hutkins, R., Sanders, M. E., Prescott, S. L., Reimer, R. A., Salminen, S. J., … Reid, G. (2017). Expert consensus document: The International Scientific Association for Probiotics and Prebiotics (ISAPP) consensus statement on the definition and scope of prebiotics. *Nature Reviews Gastroenterology & Hepatology, 14*(8), 491–502.

Gomes, J., Gomes, I., Kreiner, W., Esterbauer, H., Sinner, M., & Steiner, W. (1993). Production of high level of cellulase-free and thermostable xylanase by a wild strain of Thermomyces lanuginosus using beechwood xylan. *Journal of Biotechnology, 30*(3), 283–297.

Gong, L., Wang, H., Wang, T., Liu, Y., Wang, J., & Sun, B. (2019). Feruloylated oligosaccharides modulate the gut microbiota in vitro via the combined actions of oligosaccharides and ferulic acid. *Journal of Functional Foods, 60*, Article 103453.

Grondin, J., Tamura, K., Dejean, G., Abbott, D., & Brumer, H. (2017). Polysaccharide utilization loci: Fueling microbial communities. *Journal of Bacteriology, 199*(15).

Henrissat, B. (1991). A classification of glycosyl hydrolases based on amino acid sequence similarities. *The Biochemical Journal, 280*(2), 309–316.

Izydorczyk, M. S., & Biliaderis, C. G. (2000). Structural and functional aspects of cereal arabinoxylans and β-glucans. *Developments in Food Science, 41*(C), 361–384.

Juvonen, M., Kotiranta, M., Jokela, J., Tuomainen, P., & Tenkanen, M. (2019). Identification and structural analysis of cereal arabinoxylan-derived oligosaccharides by negative ionization HILIC-MS/MS. *Food Chemistry, 275*, 176–185.

Kaye, D. M., Shihata, W., Jama, H. A., Tsyganov, K., Ziemann, M., Kiriazis, H., … Marques, F. Z. (2020). Deficiency of prebiotic fibre and insufficient signalling through gut metabolite sensing receptors leads to cardiovascular disease. *Circulation, 141*(17), 1393–1403.

Labourel, A., Crouch, L. I., Bras, J., Jackson, A., Rogowski, A., Gray, J., … Cuskin, F. (2016). The mechanism by which arabinoxylanases can recognize highly decorated xylans. *The Journal of Biological Chemistry, 291*(42), 22149–22159.

Lagaert, S., Van Campenhout, S., Pollet, A., Bourgois, T. M., Delcour, J. A., Courtin, C. M., & Volckaert, G. (2007). Recombinant expression and characterization of a reducing-end xylose-releasing exo-oligoxylanase from Bifidobacterium adolescentis. *Applied and Environmental Microbiology, 73*(16), 5374.

Li, Z., Zhang, H., He, L., Hou, Y., Che, Y., Liu, T., … Chen, T. (2023). Influence of structural features and feruloylation on fermentability and ability to modulate gut microbiota of arabinoxylan in in vitro fermentation. *Frontiers in Microbiology, 13*.

Lin, S., Agger, J. W., Wilkens, C., & Meyer, A. S. (2021). Feruloylated Arabinoxylan and oligosaccharides: Chemistry, nutritional functions, and options for enzymatic modification. *Annual Review of Food Science and Technology, 12*(1), 331–354.

Linares-Pastén, J. A., Aronsson, A., & Karlsson, E. N. (2018). Structural considerations on the use of endo-xylanases for the production of prebiotic xylooligosaccharides from biomass. *Current Protein and Peptide Science, 19*, 48–67.

Luonteri, E., Kroon, P. A., Tenkanen, M., Teleman, A., & Williamson, G. (1999). Activity of an Aspergillus terreusα-arabinofuranosidase on phenolic-substituted oligosaccharides. *Journal of Biotechnology, 67*(1), 41–48.

Martens, E. C., Koropatkin, N., Smith, T., & Gordon, J. (2009). Complex glycan catabolism by the human gut microbiota: The bacteroidetes sus-like paradigm. *The Journal of Biological Chemistry, 284*(37), 24673–24677.

Martínez-Abad, A., Berglund, J., Toriz, G., Gatenholm, P., Henriksson, G., Lindström, M., … Vilaplana, F. (2017). Regular motifs in xylan modulate molecular flexibility and interactions with cellulose surfaces. *Plant Physiology, 175*(4), 1579–1592.

Martínez-Abad, A., Jiménez-Quero, A., Wohlert, J., & Vilaplana, F. (2020). Influence of the molecular motifs of mannan and xylan populations on their recalcitrance and organization in spruce softwoods. *Green Chemistry, 22*(12), 3956–3970.

McKee, L. S. (2017). Measuring enzyme kinetics of glycoside hydrolases using the 3,5-dinitrosalicylic acid assay. In D. W. Abbott, & A. Lammerts van Bueren (Eds.), *Protein-carbohydrate interactions*. Humana Press (pp. XIII, 311).

McKee, L. S., Peña, M. J., Rogowski, A., Jackson, A., Lewis, R. J., York, W. S., … Marles-Wright, J. (2012). Introducing endo-xylanase activity into an exo-acting arabinofuranosidase that targets side chains. *Proceedings of the National Academy of Sciences of the United States of America, 109*(17), 6537–6542.

Mendez, M. A., Pera, G., Aguclo, A., Bueno-de-Mesquita, H. B., Palli, D., Boeing, H., … Gonzalez, C. A. (2007). Cereal fiber intake may reduce risk of gastric adenocarcinomas: The EPIC-EURGAST study. *International Journal of Cancer, 121*(7), 1618–1623.

Miller, G. L. (1959). Use of dinitrosalicylic acid reagent for determination of reducing sugar. *Analytical Chemistry, 31*(3), 426–428.

Paës, G., Berrin, J.-G., & Beaugrand, J. (2012). GH11 xylanases: Structure/function/properties relationships and applications. *Biotechnology Advances, 30*(3), 564–592.

Pang, J., Zhang, Y., Tong, X., Zhong, Y., Kong, F., Li, D., … Qiao, Y. (2023). Recent developments in molecular characterization, bioactivity, and application of arabinoxylans from different sources. *Polymers, 15*.

Pastell, H., Westermann, P., Meyer, A. S., Tuomainen, P. I., & Tenkanen, M. (2009). In vitro fermentation of arabinoxylan-derived carbohydrates by bifidobacteria and mixed fecal microbiota. *Journal of Agricultural and Food Chemistry, 57*(18), 8598–8606.

Pell, G., Taylor, E. J., Gloster, T. M., Turkenburg, J. P., Fontes, C. M. G. A., Ferreira, L. M. A., … Gilbert, H. J. (2004). The mechanisms by which family 10 glycoside hydrolases bind decorated substrates. *The Journal of Biological Chemistry, 279*(10), 9597–9605.

Pereira, G. V., Abdel-Hamid, A. M., Dutta, S., D'Alessandro-Gabazza, C. N., Wefers, D., Farris, J. A., … Cann, I. (2021). Degradation of complex arabinoxylans by human colonic bacteroidetes. *Nature Communications, 12*(1), 459.

Pollet, A., Delcour, J. A., & Courtin, C. M. (2010). Structural determinants of the substrate specificities of xylanases from different glycoside hydrolase families. *Critical Reviews in Biotechnology, 30*(3), 176–191.

Pollet, A., Schoepe, J., Dornez, E., Strelkov, S., Delcour, J., & Courtin, C. (2010). Functional analysis of glycoside hydrolase family 8 xylanases shows narrow but distinct substrate specificities and biotechnological potential. *Applied Microbiology and Biotechnology, 87*(6), 2125–2135.

Pollet, A., Vandermarliere, E., Lammertyn, J., Strelkov, S. V., Delcour, J. A., & Courtin, C. M. (2009). Crystallographic and activity-based evidence for thumb flexibility and its relevance in glycoside hydrolase family 11 xylanases. *Proteins: Structure, Function, and Bioinformatics, 77*(2), 395–403.

Ray, S., Vigouroux, J., Bouder, A., Francin Allami, M., Geairon, A., Fanuel, M., … Bonnin, E. (2019). Functional exploration of Pseudoalteromonas atlantica as a source of hemicellulose-active enzymes: Evidence for a GH8 xylanase with unusual mode of action. *Enzyme and Microbial Technology, 127*, 6–16.

Rémond, C., Boukari, I., Chambat, G., & O'Donohue, M. (2008). Action of a GH 51 α- l-arabinofuranosidase on wheat-derived arabinoxylans and arabino-xylooligosaccharides. *Carbohydrate Polymers, 72*(3), 424–430.

Riviere, A., Selak, M., Lantin, D., Leroy, F., & De Vuyst, L. (2016). Bifidobacteria and butyrate-producing Colon Bacteria: Importance and strategies for their stimulation in the human gut. *Frontiers in Microbiology, 7*(979), 1–21.

Rogowski, A., Briggs, J. A., Mortimer, J. C., Tryfona, T., Terrapon, N., Lowe, E. C., … Bolam, D. N. (2015). Glycan complexity dictates microbial resource allocation in the large intestine. *Nature. Communications, 6*(1).

Rose, D. J., Patterson, J. A., & Hamaker, B. R. (2010). Structural differences among alkali-soluble arabinoxylans from maize (Zea mays), rice (Oryza sativa), and wheat (Triticum aestivum) brans influence human fecal fermentation profiles. *Journal of Agricultural and Food Chemistry, 58*(1), 493–499.

Rudjito, R. C., Ruthes, A. C., Jimenez-Quero, A., & Vilaplana, F. (2019). Feruloylated arabinoxylans from wheat bran: Optimization of extraction process and validation at pilot scale. *ACS Sustainable Chemistry & Engineering, 7*, 13167–13177.

Ruthes, A. C., Martinez-Abad, A., Tan, H.-T., Bulone, V., & Vilaplana, F. (2017). Sequential fractionation of feruloylated hemicelluloses and oligosaccharides from wheat bran using subcritical water and xylanolytic enzymes. *Green Chemistry, 19*(8), 1919–1931.

Saulnier, L., Sado, P.-E., Branlard, G., Charmet, G., & Guillon, F. (2007). Wheat arabinoxylans: Exploiting variation in amount and composition to develop enhanced varieties. *Journal of Cereal Science, 46*(3), 261–281.

Schupfer, E., Pak, S. C., Wang, S., Micalos, P. S., Jeffries, T., Ooi, S. L., … El-Omar, E. (2021). The effects and benefits of arabinoxylans on human gut microbiota – A narrative review. *Food Bioscience, 43*, Article 101267.

Singh, A. K., & Kim, W. K. (2021). Effects of dietary Fiber on nutrients utilization and gut health of poultry: A review of challenges and opportunities. *Animals, 11*(1), 181.

Smith, C. J., Rocha, E. R., & Paster, B. J. (2006). The medically important Bacteroides spp. in health and disease. In M. Dworkin, S. Falkow, E. Rosenberg, K.-H. Schleifer, & E. Stackebrandt (Eds.), *The prokaryotes* (pp. 381–427). New York, NY: Springer New York.

Snelders, J., Olaerts, H., Dornez, E., Van de Wiele, T., Aura, A.-M., Vanhaecke, L., … Courtin, C. M. (2014). Structural features and feruloylation modulate the fermentability and evolution of antioxidant properties of arabinoxylanoligosaccharides during in vitro fermentation by human gut derived microbiota. *Journal of Functional Foods, 10*, 1–12.

Sorensen, H. R., Pedersen, S., Jorgensen, C. T., & Meyer, A. S. (2007). Enzymatic hydrolysis of wheat arabinoxylan by a recombinant "minimal" enzyme cocktail containing β-xylosidase and novel endo-1,4-β-xylanase and α-L-arabinofuranosidase activities. *Biotechnology Progress, 23*(1), 100–107.

Tryfona, T., Bourdon, M., Delgado Marques, R., Busse-Wicher, M., Vilaplana, F., Stott, K., & Dupree, P. (2023). Grass xylan structural variation suggests functional specialization and distinctive interaction with cellulose and lignin. *The Plant Journal, 113*(5), 1004–1020.

Vardakou, M., Dumon, C., Murray, J. W., Christakopoulos, P., Weiner, D. P., Juge, N., … Flint, J. E. (2008). Understanding the structural basis for substrate and inhibitor recognition in eukaryotic GH11 xylanases. *Journal of Molecular Biology, 375*(5), 1293–1305.

Vardakou, M., Flint, J., Christakopoulos, P., Lewis, R. J., Gilbert, H. J., & Murray, J. W. (2005). A family 10 Thermoascus aurantiacus xylanase utilizes arabinose decorations of xylan as significant substrate specificity determinants. *Journal of Molecular Biology, 352*(5), 1060–1067.

Vardakou, M., Palop, C. N., Christakopoulos, P., Faulds, C. B., Gasson, M. A., & Narbad, A. (2008). Evaluation of the prebiotic properties of wheat arabinoxylan fractions and induction of hydrolase activity in gut microflora. *International Journal of Food Microbiology, 123*(1), 166–170.

Viëtor, R. J., Kormelink, F. J. M., Angelino, S. A. G. F., & Voragen, A. G. J. (1994). Substitution patterns of water-unextractable arabinoxylans from barley and malt. *Carbohydrate Polymers, 24*(2), 113–118.

Vos, D. D., Collins, T., Nerinckx, W., Savvides, S. N., Beeumen, V. J., Claeyssens, M., … Feller, G. (2006). Oligosaccharide binding in family 8 glycosidases: Crystal structures of active- site mutants of the beta-1,4-xylanase pXy1 from pseudoaltermonas haloplanktis TAH3a in complex with substrate and product. *Biochemistry (Easton), 45*(15), 4797.

Wang, J., Bai, J., Fan, M., Li, T., Li, Y., Qian, H., … Rao, Z. (2020). Cereal-derived arabinoxylans: Structural features and structure–activity correlations. *Trends in Food Science & Technology, 96*, 157–165.

Yao, H., Flanagan, B. M., Williams, B. A., Ismail, M., Ersya, A. D., Gidley, M. J., & Mikkelsen, D. (2023). Enzymatic arabinose depletion of wheat arabinoxylan regulates in vitro fermentation profiles and potential microbial degraders. *Food Hydrocolloids, 142*, Article 108743.

Yao, T., Deemer, D. G., Chen, M.-H., Reuhs, B. L., Hamaker, B. R., & Lindemann, S. R. (2023). Differences in fine arabinoxylan structures govern microbial selection and competition among human gut microbiota. *Carbohydrate Polymers, 121039*.

Zannini, E., Bravo Núñez, Á., Sahin, A. W., & Arendt, E. K. (2022). Arabinoxylans as functional food ingredients: A review. *Foods, 11*(7), 1026.

Zeppa, G., Conterno, L., & Gerbi, V. (2001). Determination of organic acids, sugars, diacetyl, and acetoin in cheese by high-performance liquid chromatography. *Journal of Agricultural and Food Chemistry, 49*(6), 2722–2726.

Zeybek, N., Rastall, R. A., & Buyukkileci, A. O. (2020). Utilization of xylan-type polysaccharides in co-culture fermentations of Bifidobacterium and Bacteroides species. *Carbohydrate Polymers, 236*, 116076.